THERMOMECHANICAL BEHAVIOR OF SISAL FIBERS GRAFTED WITH POLY(ACRYLAMIDE-CO-N-VINYL-2-PYRROLIDONE) AND LOADED WITH SILVER IONS OR SILVER NANOPARTICLES

Navin Chand,[a] S. K. Bajpai,[b] Ruchi Joshi,[a] and Grace Mary [b]

The graft copolymerization of acrylamide, N-vinyl-2-pyrralidone and N, N'-methylene-bis-acrylamide was carried out to modify the sisal fiber to improve its mechanical and thermal stability. The grafting of poly-(acrylamide-co-N-vinyl-2-pyrrolidone) on sisal fiber surfaces facilitated the loading of Ag(I) ions and Ag(0) nanoparticles. Surface microstructure of the surface modified sisal fiber confirmed the grafting of the copolymer. The XRD and FTIR graphs also showed changes on grafting and on Ag(I) ions and the loading of Ag(0) nanoparticles. It is evident from the DSC curves that the initial thermal stability was improved by delaying the hemicellulose decomposition on grafting and silver ion loading.

Keywords Sisal fibers; Grafting; Strength; DSC; SEM; XRD

*Contact information: a: Polymer Composite Group, Advanced Materials and Process Research Institute, Bhopal, India. b: Polymer Research Laboratory, Department of Chemistry, Government Model Science College, Jabalpur 482001, India.*Corresponding Author:- navinchand15@yahoo.co.in*

INTRODUCTION

The study and development of polymeric composite materials, especially using lignocellulosic fibers, have received increasing attention. This is interesting from the environmental and economical viewpoints, as lignocellulosic fibers such as sisal and coir are obtained from renewable resources. Sisal fiber is an important reinforcing fiber for composite applications. The surface modification of natural fibers improves the adhesion of fiber-matrix interfaces in a composite, which in turn change the mechanical properties of composites. Pongprayoon et al. (2008) carried out admicellar polymerization to modify sisal fiber surfaces with PMMA, which improved the compatibility between the sisal fiber and matrix in the composite. Tragoonwichian et al. (2007) treated sisal fibers with sodium hydroxide, γ-aminopropyltrimethoxysilane, and γ-glycidoxypropyltrimeth-oxysilane, which were then incorporated in mixture of bezoxaine and bisphenol A type epoxy resins. They found changes in the morphology, chemical groups, and hydrophilicity of the fibers. The grafting was carried out on sisal fibers with methacrylonitrile (MAN) under UV radiation to modify mechanical and degradable properties (Khan et al. 2007). Sisal fibers also were modified by a graft copolymerization reaction (Faulstich and Frollini 2006)**.** The grafting of itaconic acid onto sisal fiber by using potassium persulfate was also investigated (Naguib 2002). Radiation-induced graft copolymerizaton of ethyl acrylate onto sisal fibers was investigated. It was found that the percent added on of ethyl acrylate to sisal fibers was prohibitively low when using the direct grafting method due to excessive homopolymerization. The preradiation method

was found to be effective for improving the grafting content. In the presence of small amounts of styrene the copolymerization was achieved with little homoploymer formation by a direct grafting technique **(**Zahran and Zohdy 2003).

Fibers from natural sources, especially polysaccharides such as alginates (Knill et al. 2004), chitin and chitosan (Mattioli-Belmonte et al. 1997; Qin and Agboh 1998), and cellulose (Lee et al. 2000), etc. have been considered as the most promising dressing material. Most recently, Qin et al. (2006, 2007) have reported chitosan fibers as wound dressing material for the release of potential ions like Zn^{++}, Cu^{++}, and Ag^{+} to produce anti-microbial effect and to enhance bone-formation.

Sisal is another natural fiber obtained from the leaves of a plant (*Agave sisalana*). It is naturally found in Africa, Central America, and Florida. Sisal yields a stiff fiber and is mostly used for marine applications. It is one of the most produced natural fibers after cotton. The fiber is smooth, straight, and light yellow in colour. It is fairly coarse, and it is extensively used because of its strength, durability, ability to stretch, affinity for certain dyestuffs, and resistance to deterioration in saltwater.

The average length of sisal fiber varies from 0.6 to 1.2m; the diameter of fiber is about 0.24mm. The chemical constituents of the fiber are cellulose 66-72%, lignin 10-14%, hemicellulose 12%, and moisture 10%. The physical properties of these sisal fibers vary from source to source (Chand and Rohatgi 1986). The composition of sisal fiber is reported by Chand and Hashmi (1993). In order to improve fiber resistance towards microbial attack it is necessary to modify the surface of sisal fiber by grafting. There is no paper in the literature on the grafting of sisal fiber by acrylamide, N-vinyl-2-pyrralidone and N, N'-methylene-bis-acrylamide.

In this paper, sisal fiber was grafted by using acrylamide, N-vinyl-2-pyrralidone and N,N'-methylene-bis-acrylamide. Microstructures of grafted and plain sisal fiber were observed by using a scanning electronic microscope. Tensile strengths of grafted and plain sisal fibers were determined and compared. Thermal and dynamic mechanical behavior of grafted and plain sisal fibers were determined and compared.

EXPERIMENTAL

Materials

The sisal fibers used in the investigation were obtained from district Sieoni (M.P.), India. The monomers acrylamide (AAm) and N-vinyl-2-pyrrolidone (VP), crosslinker N,N'-methylene bisacrylamide (MB), and initiator ceric ammonium nitrate (CAN) were obtained from Himedia, Mumbai, India. The catalyst nitric acid (HNO_3) and other chemicals were also analytical grade and received from S. D. Fine Chemicals, Mumbai, India.

Grafting Procedure

All procedures, from solution preparation to the graft co-polymerization, were performed at room temperature. Both the initiator (CAN) and monomer/crosslinker were dissolved in 0.36 M HNO_3, and bubbled with N_2 gas. Pre-weighed sisal fibers were put in 50ml of 35mM CAN solution for 10min, washed with tap water to remove extra CAN,

and then immersed in 25ml of solution, containing pre-determined quantities of monomers AAm, VP, and crosslinker MB. After the graft polymerization reaction, the substrate was washed in acetone to remove homopolymer formed (Taghizadeh and Darvishi 2001) and then equilibrated in distilled water for 48h to remove unreacted salts. This step was essential to remove all unreacted monomers from the grafted product. Finally, the grafted fibers were dried at 40°C in a dust-free chamber till the fibers attained constant weight. The percent grafting (PG) was calculated using the following expression (Rout et al. 2002),

$$\%Grafting(PG) = \frac{W_g - W_o}{W_o} X100 \quad (1)$$

where W_o and W_g are the sample weights before and after graft co-polymerization, respectively.

Loading of Ag (I) Ions onto the Grafted Fibers

Pre-weighed dry fibers were put in aqueous solutions of Ag (I) ions of definite concentration. The fibers were taken out after 24h and their mass was measured using a sensitive electronic balance (Denever, TB-124). The percent-entrapment efficiency of fibers was calculated using the following empirical equation,

$$\%EntrapmentEfficiency(PEE) = \frac{WL - W_o}{W_o} X100 \quad (2)$$

where W_o and W_L are the fiber weight before and after loading.

FTIR Analysis

The FTIR-spectra of plain and grafted sisal fibers were recorded with a Shimadzu spectrometer (UV 1700) using KBr mixed disc /pallet.

SEM Analysis

The morphological features of grafted fibers were observed by using a JOEL JSM 840 A (JAPAN) scanning electron microscope. The samples were gold coated before observation.

Mechanical Testing

The stress-strain curves of plain sisal and grafted sisal fibers were obtained at room temperature on fiber testing machine LRX+LLOYD. The fibers were tested at a crosshead speed of 10 mm/min and gauge length of 50 mm. The measurements were made with four samples and average values have been reported in the data.

DMA Testing

Dynamic mechanical analysis was carried out in air with a Dynamic mechanical spectrometer model (DM 1600 SII Nanotechnology Inc.). Measurement of storage

modulus ($E^{'}$), loss modulus ($E^{''}$) and $\tan\delta$ of the samples was carried out under tensile mode at 1, 2, 5, and 10 Hz frequencies in the temperature range of 40°C to 130°C.

DSC Testing

DSC scan were recorded using a Mettler Tolledo model DSC 822e with plain and grafted sisal fibers of known weight in sealed aluminium pans. The samples were heated from 40°C to 380°C at the heating rate of 10°C/ min under a constant flow of nitrogen gas. ΔH, melting peak, and glass transition temperature (T_g) were determined.

XRD analysis

XRD analysis for plain, grafted, silver ion, and nano silver particles loaded grafted sisal fibers were performed with a Rikagu diffractometer (Cu K_α radiation, λ = 0.1546 nm) running at 40 kV and 40 mA.

RESULTS AND DISCUSSION

Sisal fiber is a yellowish fiber having high mechanical properties as compared to other natural fibers. The surface modification of sisal fiber was done by using graft copolymerization. The graft co-polymer system used in this study was comprised of a backbone material (sisal fiber in this case) to which a second polymer was attached (poly (AAm-co-VP) in this study) at reactive sites along the macromolecular chains. The mechanism of graft co-polymerization of vinyl monomers onto coir has been described by a number of workers (Gupta and Sahoo 2001; Zahran and Mahmoud 2003).

It is proposed that in this case graft copolymerization takes place by the following mechanism. In the presence of an acid used, HNO_3 (HA), primary radical species formation occurred as a result of the action of acid on Ce(IV):

$$Ce^{4+} + HA \longrightarrow Ce^{3+} + H^{+} + A^{*} \quad (3)$$

Once the free radical species (A*) are formed, they produce sisal-bound macroradicals via direct abstraction of hydrogen atoms from molecules on the sisal fibers. From this chemical formula, it is clear that free radical species (A*) are formed due to H-abstraction from major components of the sisal fiber (sisoamine, 2-deoxystreptamine, garosamine).

$$Sisal + A^{*} \longrightarrow Sisal\text{-}O^{*} + HA \quad (4)$$

where Sisal-OH represents one of the major components of sisal. From these structures, it is clear that a macroradical is forming on the surface of sisal fibre, and –OH represents a group on the surface of sisal.

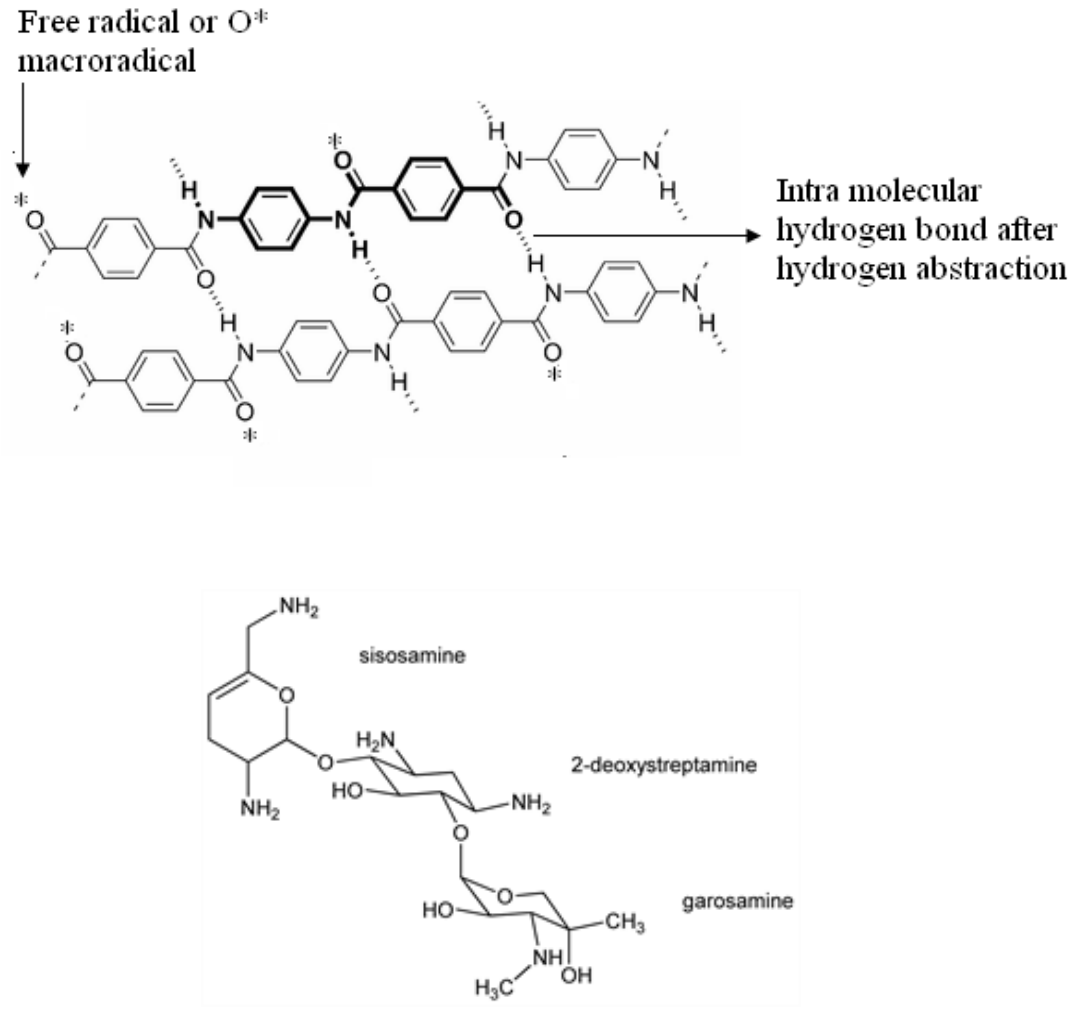

Chemical structure of sisal

The sisal macroradical would have formed by direct attack of Ce^{4+} ions on cellulose molecule via H abstraction:

$$\text{Sisal-OH} + Ce^{4+} \longrightarrow \text{Sisal-O}^{*} + Ce^{3+} + H^{+} \qquad (5)$$

When a monomer approaches one of these sisal macroradicals, a graft-copolymerization reaction can occur.

For loading of Ag (I) ions and Ag (0) nanoparticales, pre-weighed dry sisal fibers were added to aqueous solutions of Ag (I) ions of definite concentration.

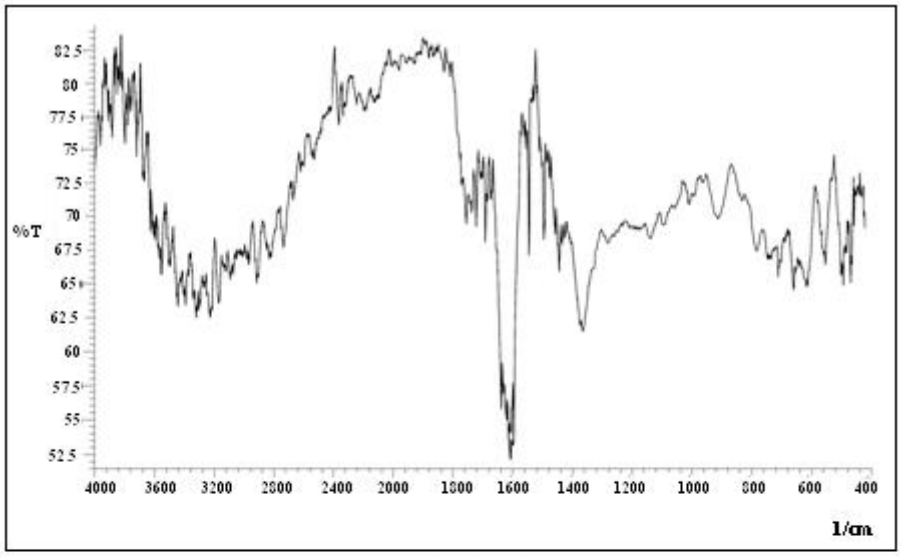

1(A)

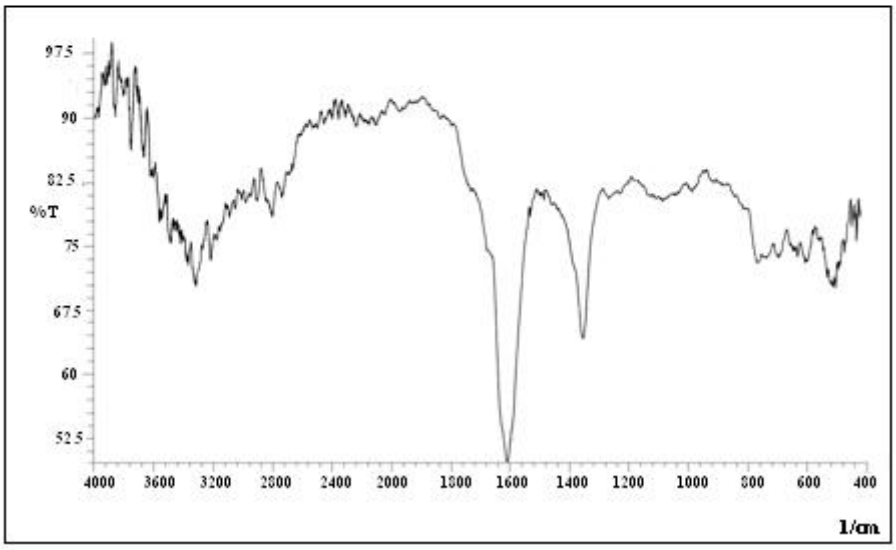

1(B)

Fig. 1. FTIR sprectra of plain sisal fiber (A) and grafted sisal fiber (B)

FTIR has been used in the past to determine the functional groups present in lignocellulosic materials. FTIR spectroscopy was used to analyze the changes that occurred in sisal fiber on modification. Figure 1 shows comparative spectra of plain and grafted sisal fibers. In Fig. 1 (A) the band located in the region 1245-1268 cm^{-1} and at 1740 cm^{-1} is for the C-O ring of lignin and carboxylic groups of pectin and hemicellulose present in plain sisal fiber. In Fig. 1 (B) the reduction of C-O ring and carboxylic groups' band is observed, which is due the grafting of co-polymer on the sisal fiber. In both the FTIR spectra (Fig. 1 (A) and (B)) there is an absorbance peak near 1430 cm^{-1}; this peak is

very similar to the absorbance peak observed between 1430-1431 cm^{-1} in kenaf pulp that was attributed to CH_2 symmetric bending (Nacos et al. 2006). The IR spectra of 1(A) and (B) clearly shows a broad band at 3350-3550 cm^{-1}, which is due to bonded OH, and symmetrical and asymmetrical stretching of C-H are found at 2890 cm^{-1} and 2760 cm^{-1}, respectively. The spectra 1(B) shows a small shifting at 3100-3200cm^{-1} due to the >C=O groups of N-vinyl-2-pyrrolidone which form the co-polymer with the amide moiety of the acrylamide. Khalil et al. (2001) also observed a peak in the 3400-3300 cm^{-1} region corresponding to the OH group.

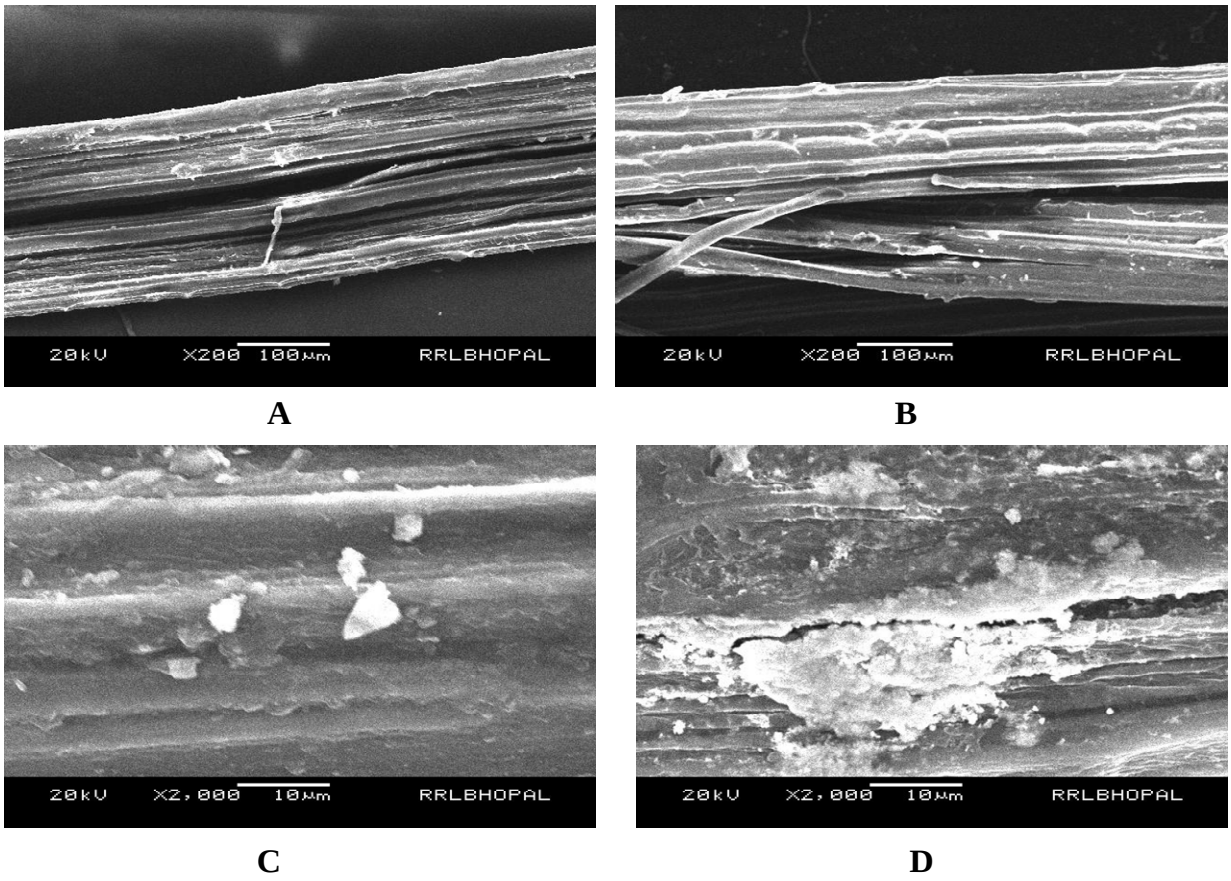

Fig. 2. SEM of plain sisal fiber (A), grafted sisal fiber (B), silver ion loaded sisal fiber (C), and silver nano loaded sisal fiber (D).

Scanning electron microscopic images of plain sisal fiber, grafted sisal fiber, silver ion loaded, and nano silver loaded sisal fibers are depicted in Fig. 2 (A-D). Figure 2 (A) shows a plain surface of the sisal fiber. This microstructure has clearly visible cells. In Fig. 2(B), a layer of polyacrylamide is observed on the surface of the sisal fiber. On the other hand, silver ions and silver nanoparticles are clearly visible on the surface of the grafted sisal fiber respectively [Fig. 2 (C) and (D)]. The reason for the presence of silver nanoparticles inside the grafted networks may be that when silver ions, present on the surface of the sisal fiber, are reduced by sodium citrate, the silver

nanoparticles, so produced, increase the gel porosity, thus providing a pathway for reducing agent to enter into the bulk to produce nanoparticles.

Table 1. Tensile Strength of Fibers

S.No.	Sample Designation	Tensile Strength (MPA)	% Elongation
1	Plain Sisal Fiber	142.7	3.05
2	Grafted Sisal Fiber	191.5	2.06
3	Silver Ion loaded Grafted Sisal Fiber	775.2	2.67
4	Silver Nano loaded Grafted Sisal Fiber	301.3	2.24

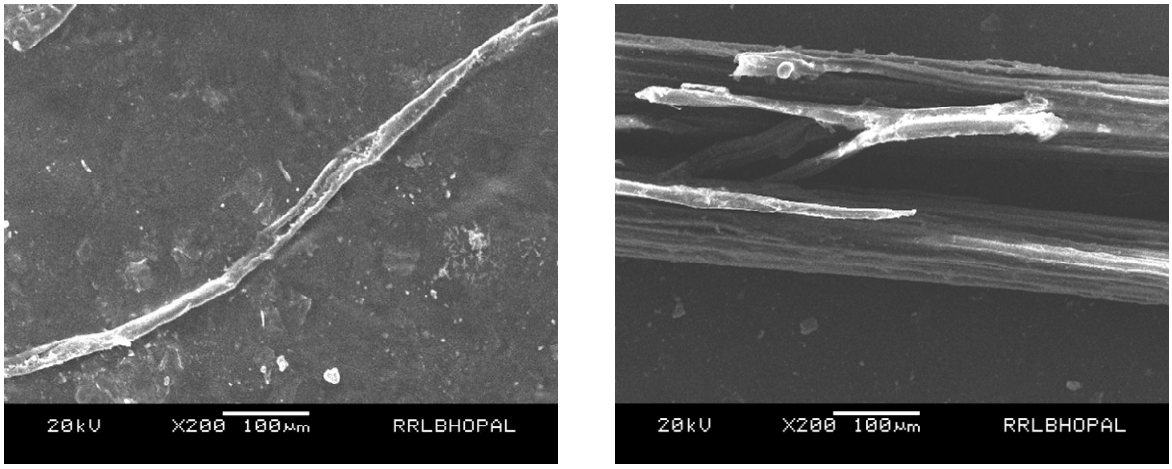

A **B**

Fig. 3. Tensile fracture SEM of plain sisal fiber (A) and grafted sisal fiber (B)

The tensile strength of grafted and plain sisal fiber was found to be 194.6MPa and 142.9MPa, respectively. Grafted sisal fiber had higher tensile strength as compared to plain sisal fiber. This was attributed to filling of the gaps present in the sisal fiber. Remarkable change in elongation of fiber was observed on grafting, as is clear from Table 1. Figure 3 (A and B) shows the magnified microstructures of the tensile-fractured surface of plain and grafted sisal fiber, respectively. A decrease in the frequency of defects in grafted sisal fiber is clearly visible in microstructure shown in Fig. 3 (B).

Figure 4 (A) shows the variation of $E^{'}$, $E^{''}$, and tan δ with temperature at 1, 2, and 10 Hz frequencies for plain sisal fiber. The $E^{'}$ remained constant at all the frequencies up to 120.0°C, except there was a small decrease around 61.0°C due to removal of volatiles. Plain sisal fiber stopped taking load after 120°C and broke. This behavior was similar to

the DSC behavior of plain sisal fiber, in which a peak occurred at 147.5. The tan δ plot shows the existence of peak at 61.1, 62.4, and at 63.4, corresponding to 1, 2, and 10 Hz.

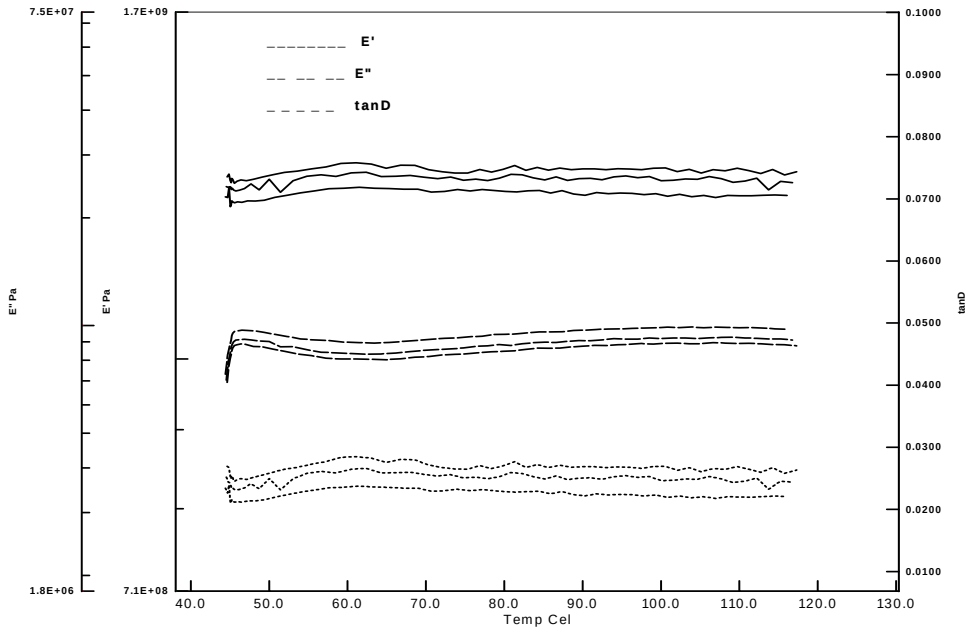

Fig. 4 (A). DMA plot of plain sisal fiber

Figure 4 (B) shows the variation of $E^{'}$, $E^{"}$, and tan δ with temperature at 1, 2, and 10 Hz frequencies for grafted sisal fiber. The tan δ peaks at 74.5, 74.0, and 74.8 ^{o}C corresponded to 1, 2, and 10 Hz. The $E^{'}$ remained constant up to 58.0°C and then increased up to 103.6, 104.6, and 105.5°C, corresponding to 1, 2, and 10 Hz frequencies. After this, the $E^{'}$ decreased due to creation of defects on removal of moisture from the grafted sisal fiber. At all the temperatures $E^{'}$ values for grafted sisal fiber were higher as compared to plain sisal fiber due to reduction in defects and pores that were present in plain sisal fiber.

Figure 4 (C) shows the variation of $E^{'}$, $E^{"}$, and tan δ with temperature at 1, 2, and 10 Hz frequencies for silver ion loaded grafted sisal fiber. The tan δ graph observed for silver ion loaded sisal fiber exhibited a peak around 75.0°C. The peaks observed at 75.7, 75.1, and 74.4°C correspond to 1, 2, and 10 Hz frequencies. It was also observed that $E^{'}$ suddenly increased around this temperature, and after that there was a gradual increase in $E^{'}$, which continued up to 109.0°C and then became nearly constant.

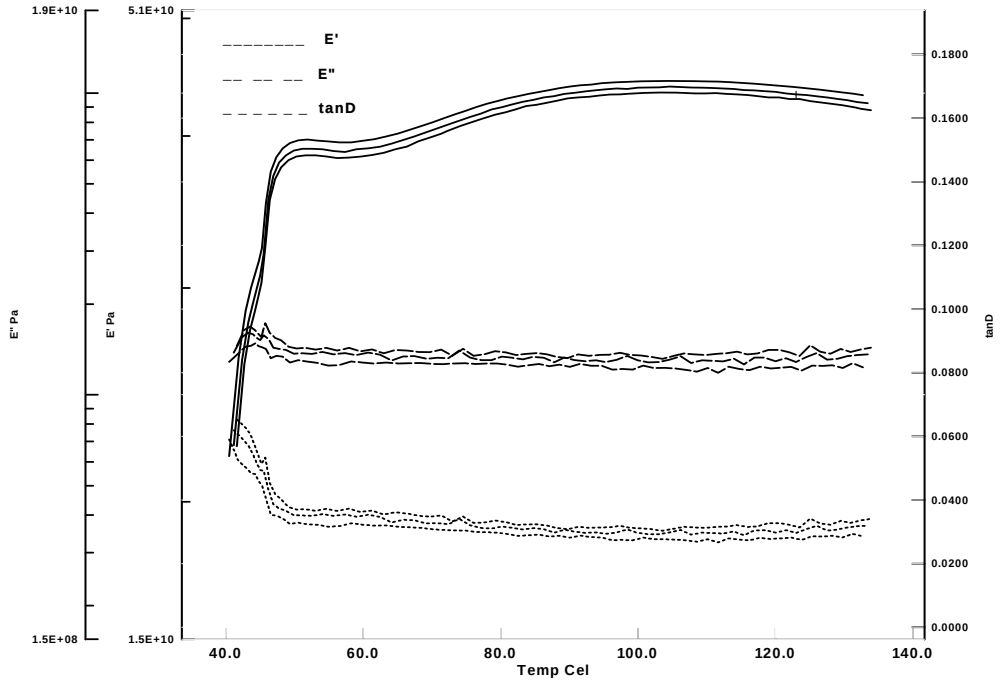

Fig. 4 (B). DMA plot of grafted sisal fiber

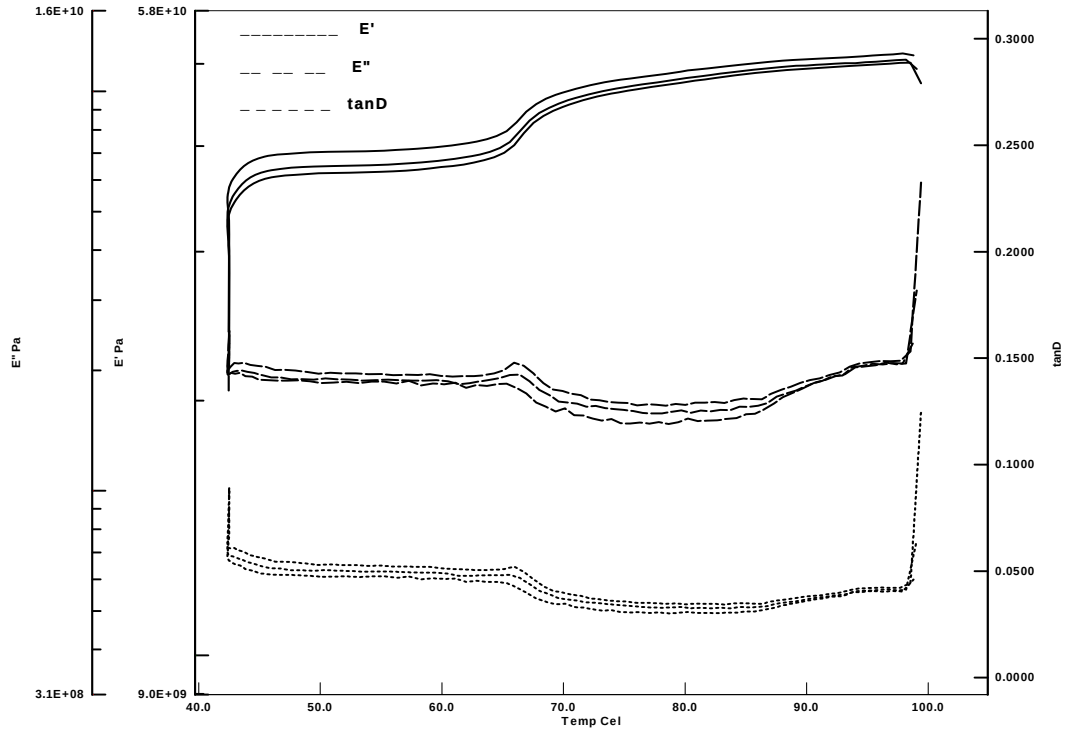

Fig. 4 (C). DMA plot of silver ion loaded grafted sisal fiber

Figure 4 (D) shows the variation of $E^{'}$, $E^{''}$, and tan δ with temperature at 1, 2, and 10 Hz frequencies for nano silver loaded sisal fiber. The $E^{'}$ plots show a maximum increase in slope at 66.7, 66.3, and 66.1°C, corresponding to 1, 2, and 10 Hz frequencies, respectively, and then the slope increased up to 90.0°C. After that, it became constant at all frequencies. The tan δ plot showed a peak around 66.7, 66.3, and 65.2°C, corresponding to 1, 2, and 10 Hz frequencies. This peak occurred due to removal of water present in sisal fiber.

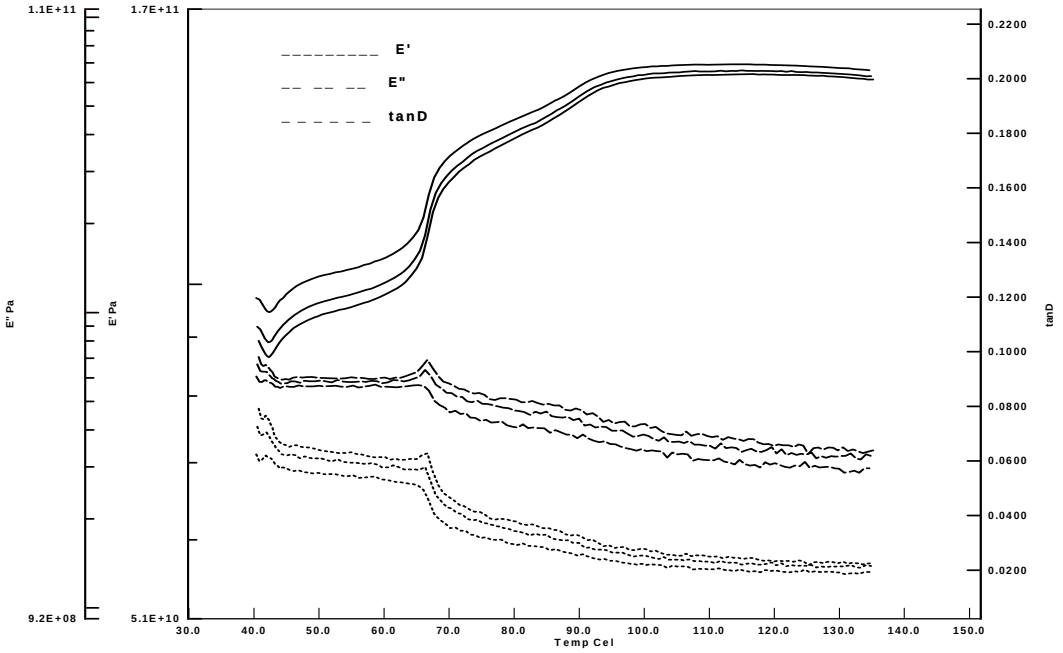

Fig. 4 (D). DMA plot of silver nano loaded grafted sisal fiber

It has been reported in the literature that dehydration as well as degradation of lignin in sisal fibre occurs in the temperature range from 60 to 200°C. In the DTG graph a peak was observed at 65°C for sisal fibre, corresponding to heat of vaporization of water from the fibre (George et al. 1996; Kazayawoko et al. 1997). Natural fibres generally lose their strength around 160°C (Akita and Kase 1967; Bash and Lewin 1973).

Thermal analyses of cellulosic fibres have been carried out, and pyrolytic behaviour was earlier reported (Bash and Lewin 1973). Depolymerization of hemi-cellulose occurs between 150 and 350°C. Random cleavage of the glycosidic linkage of cellulose takes place between 275°C and 350°C. Degradation of lignin occurs within the range 250-500°C. Akita and Kase (1967) reported that in case of lignocellulosic fibres, lignin degrades at around 200°C.

In Fig. 5 (A-D) a sharp endothermic peak is observed at around 147°C in plain sisal fiber, grafted sisal fiber, and silver nano loaded sisal fiber, while a broad endothermic peak is observed at 119.1°C in silver ion loaded sisal fiber. This may be

explained as follows: Dehydration and degradation of lignin is not affected by the grafting and silver nano loading, but silver ion loading caused dehydration and degradation of lignin at lower temperature. In the present study, peaks observed at 262.7°C and at 367.7°C correspond to two-stage decomposition of sisal fiber in air atmosphere. The presence of O_2 in air shifted the first decomposition towards lower temperature as compared to the decomposition of sisal fiber under He atmosphere, which occurred at 295°C. The second decomposition peak is due to cellulose decomposition (Fung et al. 2002).

It was observed that the hemicellulose depolymerization peak shifted to the lower temperature side on grafting, while on loading of Ag (I) ions the defects caused during the grafting were plugged, which increased the decomposition temperature, resulting in increased stability of the fiber.

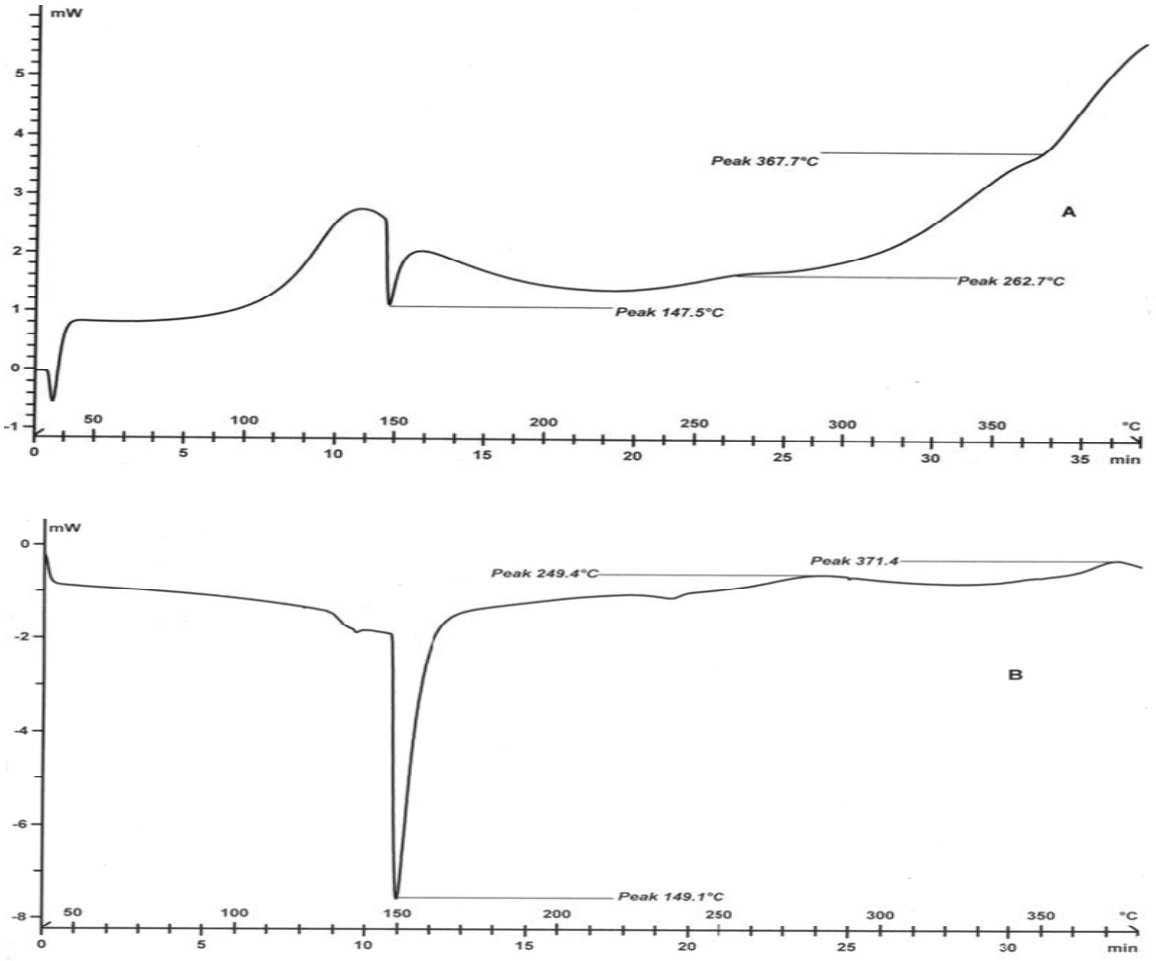

Fig. 5 (A & B). DSC scans of plain sisal fiber (A) and grafted sisal fiber (B)

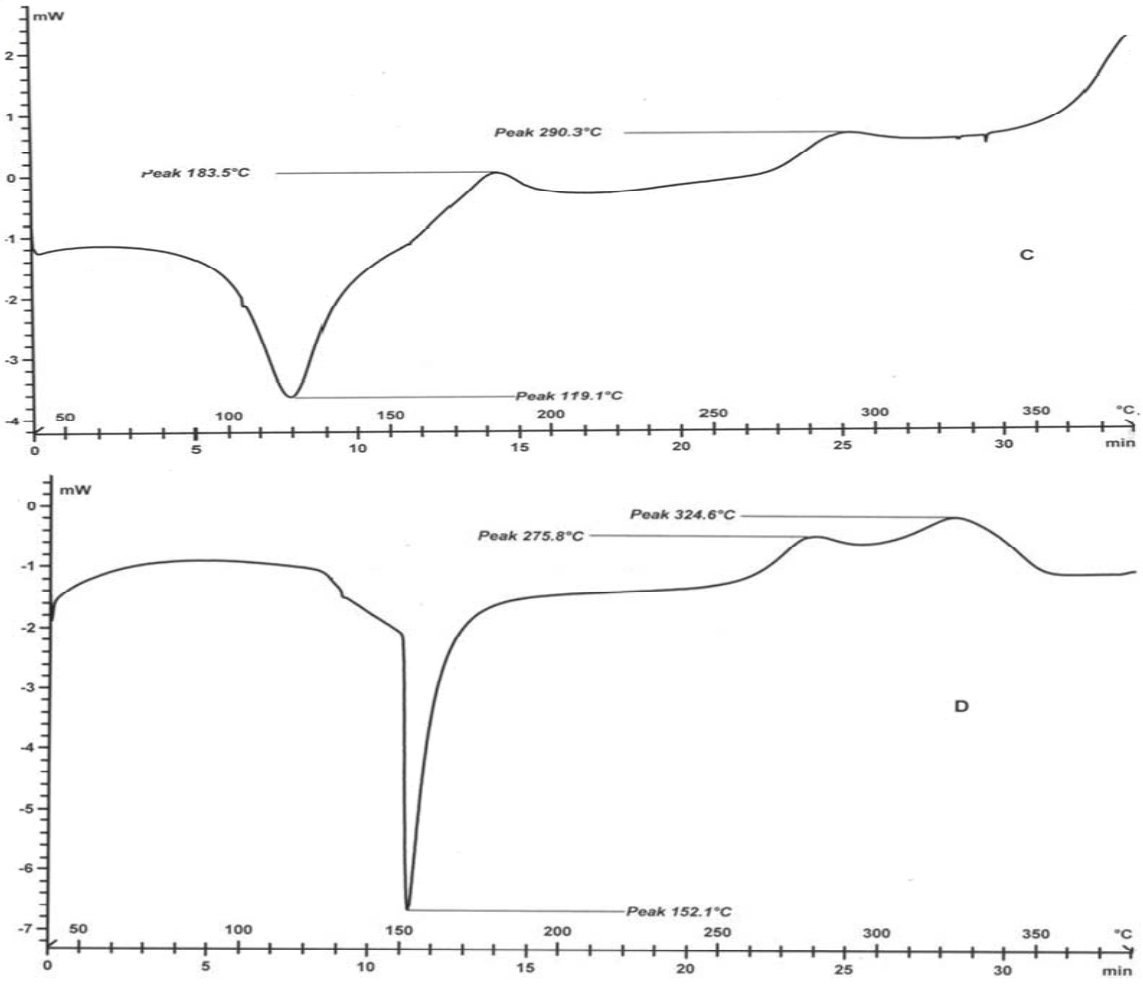

Fig. 5 (C & D). DSC scans of Ag ion loaded sisal fiber (C) and Ag nanoparticle loaded sisal fiber (D)

Table 2. DSC Data of Plain, Grafted, Siver Ion, and Silver Nano Loaded Sisal Fibers

S.No.	Sample Designation	Heating Rate (°C)	Normalized (J/g)	Peak Temperature (°C)
1	Plain Sisal Fiber	10	-47.8	147.5
			4.71	262.7
			-23.9	367.7
2	Grafted Sisal Fiber	10	-123.7	149.1
			-2.6	234.1
			5.4	371.4
3	Silver Ion loaded Grafted Sisal Fiber	10	-131.8	119.1
			10.2	183.5
			18.3	290.3
4	Silver Nano loaded Grafted Sisal Fiber	10	-131.5	152.2
			18.0	275.8
			50.7	324.6

Figure 6 (A-D) shows the XRD pattern of plain sisal fiber, grafted sisal fiber, Ag(I) ion loaded, and Ag(0) nano particles loaded sisal fiber. Plain sisal fiber exhibited three broad peaks at 10.02, 18.26, and 22.30 degrees, which are due to cellulose I (Yi et al. 2009). It is observed in Fig. 6 (B) that grafting increased the intensity of the peaks. On Ag(I) ions and Ag(0) nano loading, further increase in the intensity occurred at the 10.02 degree peak. This shows an increase in the crystalline component. On nanarticle addition an additional peak at around 38.06 degrees was occurred. Therefore, it is very clear that a silver nano loaded grafted sisal fiber contains silver nano particles.

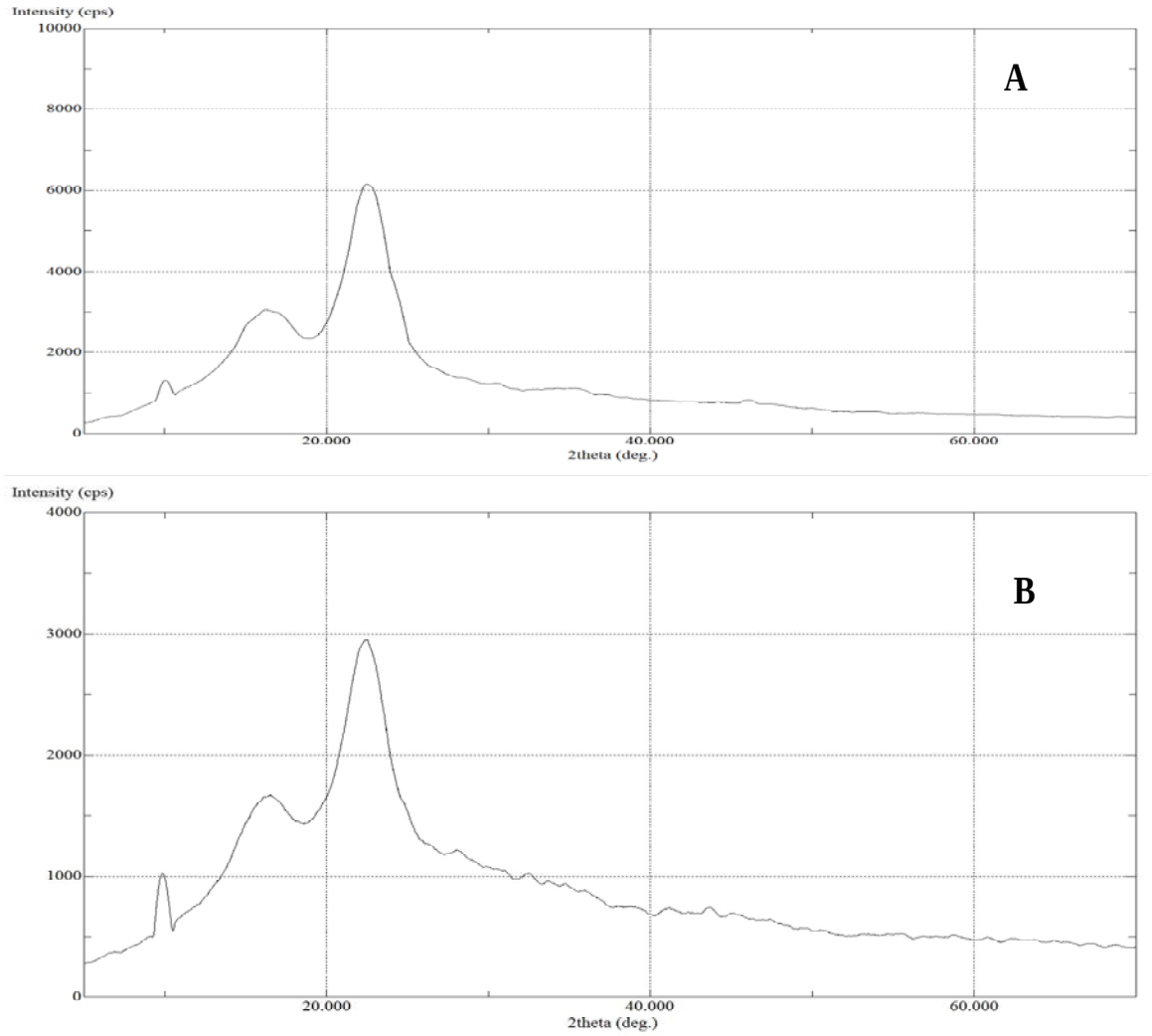

Fig. 6 (A & B). XRD of plain sisal fiber (A) and grafted sisal fiber (B)

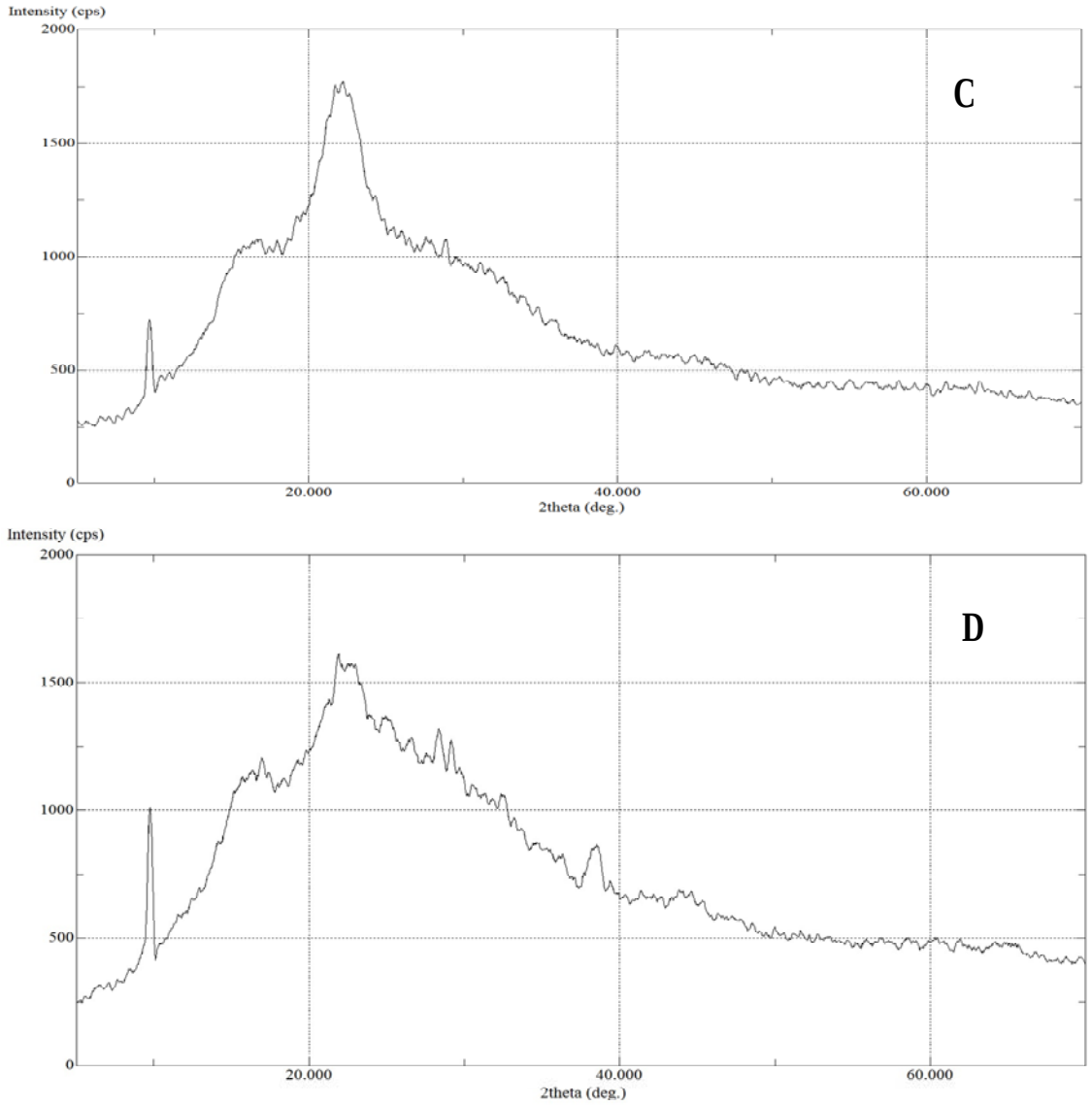

Fig. 6 (C & D). XRD of Ag ion loaded sisal fiber (C) and Ag nano particles loaded sisal fiber (D)

CONCLUSIONS

1. Sisal fibers could be grafted, with the formation of poly-(acrylamide-co-N-vinyl-2-pyrrolidone).
2. Grafting, silver ion loading, and nano loading improved the initial thermal stability of the sisal fiber.
3. The tensile strength increased on grafting and silver ion loading.
4. The grafted sisal fiber exhibited higher storage modulus values.

ACKNOWLEDGEMENT

The authors thank Dr. O.P. Sharma, Head of the Department of Chemistry, Govt. Model Science College (Jabalpur), India, for providing facilities to complete the work.

REFERENCES CITED

Akita, K., and Kase, M. (1967). "Determination of kinetic parameters of pyrolysis of cellulose and cellulose treated with ammonium phosphate by different thermal analysis and thermal gravimetric analysis," *J. Polym. Sci. A-I* 5, 833-848.

Bash, A., and Lewin, M. (1973). "Thermal analysis of cellulosic fibers," *J. Polym. Sci. Polym. Chem. Edn*. 11, 3071.

Chand, N., and Hashmi, S. A. R. (1993). "Mechanical properties of sisal fiber at elevated temperatures," *J. Mater. Sci.* 28, 1573-4803.

Chand, N., and Rohatgi, P. K. (1986). "Adhesion of sisal fibre-polyester system," *Polym. Commun.* 27, 157-160.

Faulstich de, P., and Frollini, E. (2006). "Unmodified and modified surface sisal fibers as reinforcement of phenolic and lignophenolic matrices composites: Thermal analysis of fibers ande composites," *Macromol. Mater. Eng.* 291 (4), 405-417.

Fung, K. L., Li, R. K. Y., and Tjong, S. C. (2002). "Interface modification on the properties of sisal fiber-reinforced polypropylene composites," *J. Appl. Polym. Sci.* 85, 169-176.

George, J., Bhagawan, S. S., and Thomas, S. (2004). "Thermogravimetric and dyanamic mechanical thermalanalysis of pineapple fibre reinforced polyethylene composites," *J. Thermal Anal. and Calorm.* 47(4), 1121-1140.

Gupta, K. C., and Sahoo, S. (2001). "Grafting of acrylonitrile and methyl methacrylate from their binary mixtures on cellulose using ceric ions," *J. Appl. Polym. Sci*. 79(5), 767-778.

Kazayawoko, M., Balatinecz, J. J., and Woodhams, R. T. (1997). "Diffuse relectance fourier transform infrared spectra of wood fibres treated with maleated polypropylene," *J. Polym. Sci.* 66, 1163-1173.

Khalil, H. P. A., Ismail, H., Rozman, H. D., and Ahmad, M. N. (2001). "The effect of acetylation on interfacial shear strength between plant fiber and varios matrices," *Eur. Polym. J.* 37(5), 1037-1045.

Khan, M. A., Masudul, H. M., Jasmin, A. R. A., and Mustafa, A. I. (2007). "Surface modification of sisal (*Agavae sisalana*) fiber by photocuring: Effect of additives," *Polymer-plastics Technology and Engineering*, 46(4-6), 447-453.

Knill, C. J., Kennedy, J. F., Mistry, J., Smart, G., Miraftab, M., Groocock, M. R., and Williams, H. J. (2004). "Aliginate fibers modified with unhydrolysed and hydrolysed chitosans for wound dressing," *Carbohyd. Polym.* 55 (1), 65-76.

Lee, M. H., Yoon, K. J., and Kon, S.-W. (2000). "Grafting onto cotton fiber with acrylamidomethylated beta-cyclodextrin and its application," *J. Appl. Polym. Sci*. 78 (11), 1986-1991.

Nacos, M., Katapodis, P., Daferera, D., Trantilis, P. A., Christakopoulos, P., and Polissiou, M. (2006). "Kenaf xylan-A source of biologically active acidic oligosaccharides," *Carbohyd. Polym.* 66(1), 126-134.

Naguib, H. F. (2002). "Chemically induced graft copolymerization of itaconic acid onto sisal fibers," *J. Polym. Res.* 9(3), 207-211.

Pongprayoon, T., Yanumet, N., and Sangthong, S. (2008). "Surface behavior and film formation analysis of sisal fiber coated by poly(methyl methacrylate) ultrathin film," *Colloids and Surfaces A: Physicochemical and Engineering Aspects* 320(1-3), 130-137.

Qin, Y., and Agboh, O. C. (1998). "Chitin and chitosan fibers: Unlocking their potential," *Medical Device Technol.* 9 (10), 24-28.

Qin, Y., Zhu, C., Chen, J., Chen, Y., and Zhang, C. (2006). "The absorption and release of silver and zinc ions by chitosan fibers," *J. Appl. Polym. Sci*. 101(1), 766-771.

Qin, Y. M., Zhu, C. J., Chen, J., Liang, D., and Wo, G. F. (2007). "Absorption and release of zinc and copper ions by chitosan fibers," *J. Appl. Polym. Sci*. 105 (2), 527-532.

Rout, J., Misra, M., Tripathi, S. S., Nayak, S. K., and Mohanty, A. K. (2002). "Surface modification of coir fibers. II. Cu (II)-IO4-Initiated graft copolymerization of acrylonitrile onto chemically modified coir fiber," *J. Appl. Polm. Sci*. 84, 75-82.

Taghizadeh, M. T., and Darvishi, M. A. (2001). "Kinetics and mechanism of hetrogeneous graft p[olymerization of acrylonitrile onto polyvinyl alcohol," *Iran. Polym. J*. 10 (5), 283-292.

Tragoonwichian, S., Yanumet, N., and Ishida H. (2007). "Effect of fiber surface modification on the mechanical properties of sisal fiber-reinforced benzoxaine/epoxy composites based on aliphatic diamine benzoxaine," *J. Appl. Polym. Sci.*, DOI 10.1002/app.25797.

Yi, C., Tian, L., Tang, F., Wang, L., Zou, H., and Xu, W. (2009). "Crystalline transition behavior of sisal in cycle process," *Polym. Compos.* DOI 10.1002/pc.20885.

Zahran, A. H., and Zohdy, M. H. (2003). "Effect of radiation chemical treatment on sisal fibers, radiation induced grafting of ethyl acrylate," *J. Appl. Polym. Sci*. 31(6), 1925.

Zahran, M. K., and Mahmoud, R. I. (2003). "Peroxydiphosphate – metal ion – cellulose thiocarbonate redox system induced graft copolymerization of vinyl monomer onto cotton fabric," *J. Appl. Polym. Sci*. 87, 1879-1888.

Article submitted: Sept. 13, 2009; Peer review completed: Dec. 2, 2009; Revised version received and accepted: Jan. 1, 2010; Published: Jan4, 2010.